

Reinforcement learning architecture for automated quantum-adiabatic-algorithm design

Jian Lin,¹ Zhong Yuan Lai,¹ and Xiaopeng Li^{1,2,*}

¹State Key Laboratory of Surface Physics, Institute of Nanoelectronics and Quantum Computing,
and Department of Physics, Fudan University, Shanghai 200433, China

²Collaborative Innovation Center of Advanced Microstructures, Nanjing 210093, China

(Dated: June 20, 2022)

Quantum algorithm design lies in the hallmark of applications of quantum computation and quantum simulation. Here we put forward a deep reinforcement learning (RL) architecture for automated algorithm design in the framework of quantum adiabatic algorithm, where the optimal Hamiltonian path to reach a quantum ground state that encodes a computation problem is obtained by RL techniques. We benchmark our approach in Grover search and 3-SAT problems, and find that the adiabatic algorithm obtained by our RL approach leads to significant improvement in the success probability and computing speedups for both moderate and large number of qubits compared to conventional algorithms. The RL-designed algorithm is found to be qualitatively distinct from the linear algorithm in the resultant distribution of success probability. Considering the established complexity-equivalence of circuit and adiabatic quantum algorithms, we expect the RL-designed adiabatic algorithm to inspire novel circuit algorithms as well. Our approach offers a recipe to design quantum algorithms for generic problems through a machinery RL process, which paves a novel way to automated quantum algorithm design using artificial intelligence, potentially applicable to different quantum simulation and computation platforms from trapped ions and optical lattices to superconducting-qubit devices.

Quantum simulation and quantum computing have received enormous efforts in the last two decades owing to their advantageous computational power over classical machines [1–4]. In the development of quantum computing, quantum algorithms with exponential speedups have long been providing driving forces for the field to advance, with the best known example from factorizing a large composite integer [5]. In applications of quantum advantage to generic computational problems, quantum algorithm design plays a central role. In recent years, both threads of gate-based [6] and adiabatic annealing models [7, 8] of quantum computing have witnessed rapid progress in hardware developments such as superconducting [9–14], photonic [15–17] and atomic [18–20] quantum devices. Computational complexity equivalence between the two approaches have been established in theory [21–23].

In adiabatic quantum computing, the Hamiltonian can be written as a time-dependent combination of initial and final Hamiltonians, H_B and H_P [7, 8], as

$$H = (1 - s(t/T))H_B + s(t/T)H_P, \quad (1)$$

with the computational problem encoded in the ground state of H_P . Under this framework, the quantum algorithm design corresponds to the optimization of the Hamiltonian path or more explicitly the time sequence of $s(t)$. Different choices for the path could lead to algorithms having dramatically different performance and even in the complexity scaling. For example in Grover search, a linear function of $s(t/T)$ leads to an algorithm

with a linear complexity scaling to the search space dimension (N), whereas a nonlinear choice could reduce the complexity to \sqrt{N} [24]. This implies an approach of automated quantum adiabatic algorithm design through searching for an optimal Hamiltonian path, which may lead to a generic approach of automated algorithm design given the established complexity equivalence between gate-based and adiabatic models [21–23]. The automated quantum algorithm design that is adaptable to moderate-qubit-numbers is particularly in current-demand considering near term applications of noisy intermediate size quantum devices [25].

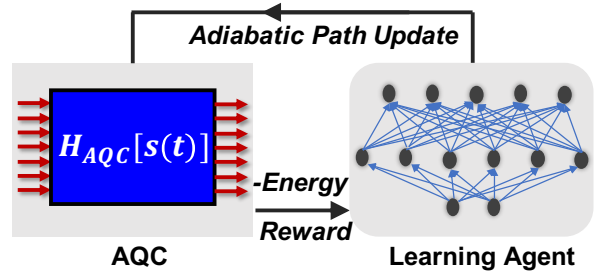


FIG. 1. Schematic illustration of the reinforcement learning (RL) approach for adiabatic quantum algorithm design. The RL agent takes the negative of the final quantum state energy of the adiabatic quantum computer (AQC) as a reward. The agent produces an action of adiabatic-path-update of $s(t)$ to optimize the reward based on its Q-table represented by a neural network.

Here, we propose a deep reinforcement learning (RL)

architecture for automated design of quantum adiabatic algorithm. By encoding the computation problem in a Hamiltonian groundstate problem, we find that the automated design of quantum algorithm can be reached by RL of the optimal Hamiltonian path. In application to the Grover search and 3-SAT problems, we find that the adiabatic algorithm designed by the machine has a better performance in terms of computing efficiency or the success probability. The RL-designed quantum algorithm is found to have emergent transferability—the algorithm obtained by training on a subset of problem instances is applicable to other very different ones while maintaining the high computational performance. This transferability is not only conceptually novel but also practically crucial in saving computation resources for training.

Results

Reinforcement learning architecture for quantum adiabatic algorithm design. Given a computational problem, e.g., Grover search or 3-SAT, the form of the Hamiltonian H_P encoding the problem is fixed. For different problem instances, for example in targeting different states in Grover search or finding solutions for different choices of clauses in 3-SAT, the encoding Hamiltonian is different. We label different problem instances by PI , and the encoding Hamiltonian is correspondingly labeled as H_{PI} . The designed Hamiltonian path in general would depend on the computational problem, for example whether it is Grover search or 3-SAT, but it should be required that the Hamiltonian path should be independent of the problem instance PI , in order for this Hamiltonian path design to make a quantum adiabatic algorithm generically applicable. This makes it distinct from path optimization aiming for preparation of specific quantum states [26] or for achieving robust or fast gate operations [27–30].

We propose an approach for automated algorithm design based on reinforcement learning (see Fig. 1 for an illustration). In the framework of quantum adiabatic algorithm, the task of algorithm design reduces to the exploration of the optimal path $s(t/T)$, which we parameterize as

$$s\left(\frac{t}{T}\right) = \frac{t}{T} + \sum_{m=1}^C b^{(m)} \sin\left(\frac{m\pi t}{T}\right). \quad (2)$$

Here C is a cutoff for high frequency components, and the parameters $b^{(m)}$ form a vector \mathbf{b} . This parametrization is asymptotically complete as the cutoff C approaches infinity.

To build an artificial intelligent agent that explores the path-space of \mathbf{b} , we introduce a set of action, \mathbf{a} , which are

defined to update \mathbf{b} as $a^{(0)}(\mathbf{b}) = \mathbf{b}$ and $[a^{(2m-1)}(\mathbf{b})]_n = b_n - \Delta\delta_{mn}$, $[a^{(2m)}(\mathbf{b})]_n = b_n + \Delta\delta_{mn}$ for $m \geq 1$. The reward, $r(\mathbf{b})$, collected by the agent is assigned to be the opposite of the final quantum state energy following the Hamiltonian (Eq. (1)) evolution given by \mathbf{b} . To target an optimal adiabatic algorithm with robust performance to all problem instances, we sample PI and average over a certain number of instances (MI) in calculating the reward for an action a on \mathbf{b} . In the reinforcement learning approach, during an intermediate j -th step, the agent evaluates the action a on \mathbf{b} according to a Q-table

$$Q^*(\mathbf{b}, a) = \max_{\pi} \mathbb{E} \left[\sum_{i=0}^{\infty} \gamma^i r(\mathbf{b}_{j+i}) | \pi \right]. \quad (3)$$

This maximizes the expected cumulative future reward by choosing an action-selecting policy $\pi = P(a|\mathbf{b})$ that describes the probability of performing the action a on a path-state \mathbf{b} . In our method, although the selection of the action is probabilistic, the next step path-state \mathbf{b}_{j+1} is deterministically set by the j -th step action and path-state, a_j and \mathbf{b}_j . In accounting for the future reward, the $(j+i)$ -th step reward is discounted by a factor of γ^i . This Q-table can be solved by iteration according to the Bellman equation [31], $Q^*(\mathbf{b}, a) = [r(a(\mathbf{b})) + \gamma \max_{a'} Q^*(a(\mathbf{b}), a')]$.

Our method uses a deep neural network to approximate the Q-table, as $Q^*(\mathbf{b}, a) \approx Q(\mathbf{b}, a; \theta)$, with θ the network parameters determined in an iterative learning process (see Methods). To stabilize the nonlinear iteration in learning, we adopt an experience-replay approach [32] where the agent's experiences $(\mathbf{b}_j, a_j, r_j, \mathbf{b}_{j+1})$ [with $r_j \equiv r(\mathbf{b}_{j+1})$] are stored in a memory \mathcal{M} with a capacity CAP . We have a network $Q(\mathbf{b}, a; \theta)$ trained *on-the-fly* during the agent exploring the path-state space. As for the neural network training, the inputs and outputs are \mathbf{b} and $r + \gamma \max_{a'} Q(\mathbf{b}' = a(\mathbf{b}), a'; \theta_-)$, respectively, with \mathbf{b} , r , and a drawn randomly from the memory \mathcal{M} , and $Q(\mathbf{b}', a'; \theta_-)$ a separate network whose parameters θ_- are updated to θ every W steps (see details in Methods).

Given the limitations of quantum computing hardwares presently accessible, we simulate quantum computing on a classical computer and generate reward to train the RL network. In applications to a quantum computer, our RL architecture for automated algorithm design is directly adaptable by collecting reward generated from a quantum computer, say with quantum phase estimation [6].

Performance in Grover search. In application of our RL approach to automated adiabatic algorithm design, we first show its performance on Grover search compared to known quantum algorithms. This search problem is to find an element in an array of length N as an

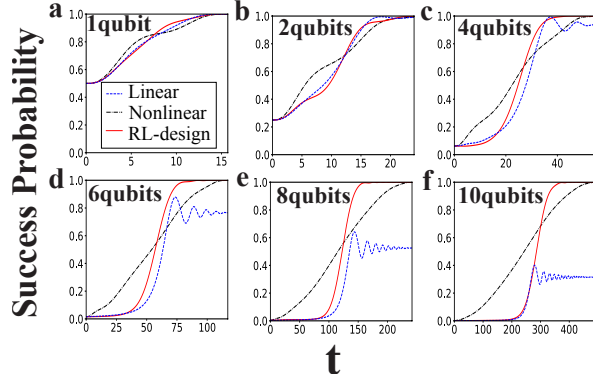


FIG. 2. Performance of RL-designed quantum adiabatic algorithm in success probability for Grover search. The success probability is obtained by taking the wave-function overlap of the dynamical quantum state with search-target state. Results from adiabatic algorithms using a linear and a tailored nonlinear path [24] are shown for comparison. The total adiabatic time are chosen to be $T = 16, 24, 55, 117, 242, 493$ for qubit number $n = 1, 2, 4, 6, 8, 10$, respectively, following the $\sqrt{N} = \sqrt{2^n}$ scaling. The machinery adiabatic algorithm designed by RL shows significant improvement over the linear algorithm, and reveals the same computation-complexity scaling as the nonlinear algorithm.

input to a black-box function that produces a particular output value. This classical problem can be encoded as searching in the Hilbert space of $n = \log_2 N$ qubits for a target quantum state. These qubits are labeled by q in the following. A circuit-based quantum algorithm was firstly designed by Grover, which shows a quadratic quantum speedup over classical computing [33]. In adiabatic quantum computing, the Hamiltonians in Eq. (1) for Grover search are $H_B = \mathbb{1} - |\psi_0\rangle\langle\psi_0|$, and $H_P = \mathbb{1} - |m\rangle\langle m|$, where $|m\rangle$ is a product state in Pauli-Z basis that encodes the search target, and $|\psi_0\rangle$ is a product state in the Pauli-X basis with all n eigenvalues equal to 1. The symbols X , Y , and Z refer to Pauli matrices in this work. A linear function choice of $s(t/T)$ ($b = 0$ in our notation), does not exhibit the quadratic speedup. It was later pointed out in Ref. 24 that the quantum speedup is reached with a tailored nonlinear path choice of $s(t/T)$.

In the Grover search problem, different problem instances correspond to different choices for the $|m\rangle$ states, which are all connected to each other by a unitary transformation $\otimes_{\{q\}} X_{\{q\}}$ for a subset of qubits $\{q\}$, which keeps H_B invariant. The reward the RL-agent collects in the training process is thus exactly the same for different problem instances, which means averaging over PI is unnecessary for the Grover search. Fig. 2 shows results of the RL-designed adiabatic Grover search algorithm.

The success probability is obtained by taking the wave function overlap of the time-dependent dynamical state with the targeted ground state that encodes the solution of Grover search. In our RL design for adiabatic quantum algorithm, we scale up the adiabatic time T as $T \propto \sqrt{N}$ to benchmark against the best-known Grover search algorithm. Then as expected, the linear adiabatic algorithm leads to a success probability completely unsatisfactory at large N . We find that both the nonlinear [24] and the RL-designed adiabatic algorithms produce success probabilities very close to 1 (larger than $\approx 99\%$). At large $N \geq 2^4$, the RL-designed algorithm outperforms the nonlinear one. The required adiabatic time T to reach a fixed success probability is shorter from the RL-designed algorithm. The computational complexity of the RL-designed adiabatic algorithm is thus expected to follow the \sqrt{N} scaling, which is known to be optimal for Grover search [34].

We further look into the RL-designed Hamiltonian path and the resultant instantaneous energy spectrum (Fig. 3). A common feature of the RL-learned path for $s(t/T)$ is that there is a relatively flat region around $s = 0.5$ where the energy gap is minimal (Fig. 3(a)). This flat region has a tendency to grow as we increase N . The instantaneous energy following the RL-designed algorithm lies on the time-dependent ground state for both small and large number of qubits (Fig. 3(b,c)). The energy deviation is much smaller than the linear algorithm, and is very close to the tailored nonlinear algorithm. Therefore the RL-design approach indeed automatically reveals a quantum adiabatic algorithm as efficient as the improved nonlinear algorithm for Grover search [24].

It is worth remarking here that the choice of H_B is made for comparison purposes, as the nonlinear path to achieve the quadratic speedup is only analytically available with that specific Hamiltonian choice [24]. In terms of realization of H_B , which is equivalent to $H_B = \mathbb{1} - \otimes_q [1 + X_q]/2$, it is experimentally challenging to construct this Hamiltonian with quantum annealing devices. A more suitable choice for H_B in that regard is $\sum_q [\mathbb{1} - X_q]$, for which the analytically obtained nonlinear path [24] is then no longer applicable, but our RL design still produces high-performance adiabatic algorithms.

Performance in 3-SAT. We then apply the RL approach to the more complicated 3-SAT problem. Given a total number of N_b boolean bits (labeled by q), the problem is to find a boolean sequence z_q to satisfy

$$C = C_1 \wedge C_2 \wedge C_3 \wedge C_4 \wedge \dots$$

with each C_i a clause containing three boolean bits, say $q_{i,k=1,2,3}$. The total clause and bit numbers will be de-

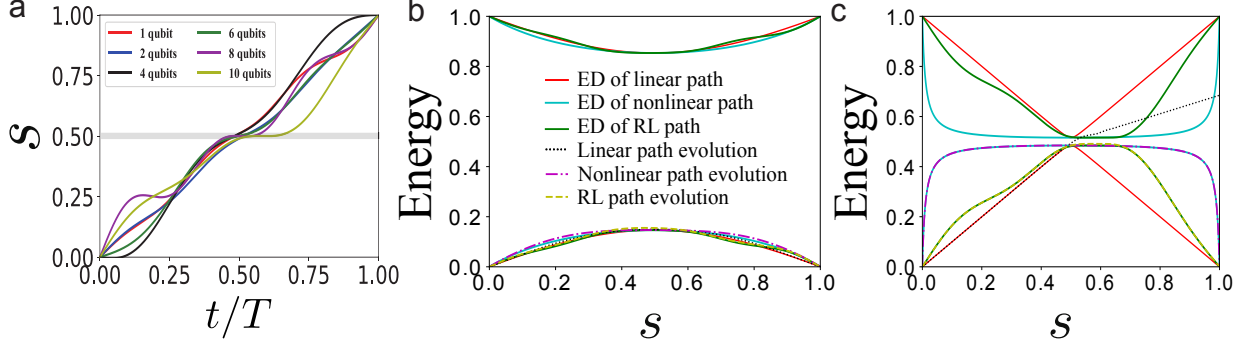


FIG. 3. Energy evolution from the RL-designed adiabatic path for Grover search. (a) shows the RL-designed path. The adiabatic time is chosen the same way as in Fig. 2. (b) and (c) show the energy spectrum for the ground and first excited states with 1 and 10 qubits, respectively. The energy spectra of the instantaneous Hamiltonian are obtained by exact diagonalization (ED), shown by ‘solid’ lines in (b, c). The plot in (c) shares the same legend as in (b). The energy expectation values of the dynamical state following different Hamiltonian paths are shown by ‘dashed’ lines. It is evident from (c) that the RL-designed path is distinct from both of the linear and the nonlinear paths.

noted as N_C . The satisfiability condition of each clause C_i can be written into a truth table $\mathbf{z}_{i\alpha} = \{z^{(1)}, z^{(2)}, z^{(3)}\}$ such that the binary sequence $\{z^{(1)}, z^{(2)}, z^{(3)}\}$ belongs to this table if and only if C_i is satisfied. We use α to label all possibilities to satisfy the clause C_i . To solve this problem with quantum adiabatic algorithm, we need to introduce N_b qubits, which are then also labeled by q . The corresponding qubit states are $|z_1\rangle \otimes |z_2\rangle \otimes \dots \otimes |z_{N_b}\rangle$. Introducing a compact notation $|\mathbf{q}_i; \mathbf{z}_{i\alpha}\rangle$ for the qubits, $q_{i,1}$, $q_{i,2}$, and $q_{i,3}$, in the quantum state $|z^{(1)}\rangle \otimes |z^{(2)}\rangle \otimes |z^{(3)}\rangle$, the classical 3-SAT problem is formally encoded into a quantum ground state problem with a Hamiltonian

$$H_P^{\text{SAT}} = - \sum_{i=1}^{N_C} \sum_{\alpha} |\mathbf{q}_i; \mathbf{z}_{i\alpha}\rangle \langle \mathbf{q}_i; \mathbf{z}_{i\alpha}|. \quad (4)$$

A solution to the 3-SAT problem corresponds to a ground state of H_P^{SAT} with energy $-N_C$. Different 3-SAT problem instances correspond to different choices of clause \mathbf{q}_i and truth table $\mathbf{z}_{i\alpha}$. The initial quantum state and Hamiltonian H_0 are set to be $H_0 = \sum_q [\mathbb{1} - X_q]/2$. In our RL approach to design 3-SAT quantum algorithm, the reward RL-agent collects is generated by randomly sampling \mathbf{q}_i and $\mathbf{z}_{i\alpha}$ (see Method), to make the learned algorithm generically applicable.

In Fig. 4, we show the performance of the RL-designed algorithm and compare with the linear algorithm. We put the RL-agent to work on a 10-bit 3-SAT problem. The RL-designed algorithm is obtained by training with clause number $N_C = 3$ only, where the stepwise reward is obtained by averaging over 100 random problem instances. We then test the RL algorithm on random 3-SAT problem instances that contain one-to-six clauses. The

tested success probability in Fig. 4(a) is obtained by averaging over 10^5 random problem instances. It is evident that the RL-designed algorithm outperforms the linear algorithm with higher success probability. Its advantage becomes more significant in a systematic fashion as the clause number is increased, although the RL algorithm is trained on 3-SAT problems with clause number $N_C = 3$ only, implying the transferability of the RL-designed algorithm. The success over different clause numbers implies that this RL-learning approach has seized the intrinsic ingredients to optimize the adiabatic quantum algorithm because otherwise the RL-designed algorithm would not be transferable.

Besides the quantitative improvement in the RL-designed over the linear algorithm, we also emphasize that the outcome of the RL algorithm is qualitatively distinct in the resultant fidelity. In Fig. 4(b, c), we show the distribution of the infidelity obtained from 10^5 random 3-SAT problem instances. The statistics is taken for different clause number separately. The infidelity is rescaled by taking its average as a unit. The distributions of this rescaled infidelity for different clause numbers are found to collapse onto a universal function, for both the RL (Fig. 4(b)) and linear (Fig. 4(c)) algorithms. It is evident that infidelity distribution from the linear algorithm is close to a Wigner-Dyson (WD) distribution—the numerically obtained statistical second moment of the infidelity agrees with the WD prediction within 10% difference. To the contrast, the second moment of the infidelity from the RL algorithm strongly deviates from the WD prediction, meaning the infidelity distribution for the RL algorithm is qualitatively distinctive from the linear case.

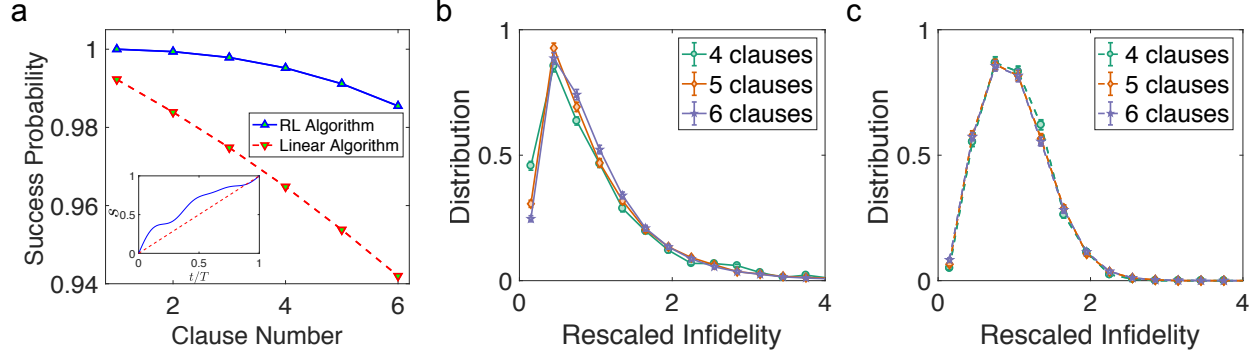


FIG. 4. Performance of reinforcement learning (RL) designed algorithm on 3-SAT problem. In (a), we show the comparison of the RL-designed and linear algorithms in the averaged success probability of solving random 3-SAT problems. The success probability is defined by projecting the final state of the adiabatic quantum evolution onto the correct solutions. (b) and (c) show the distribution of the infidelity for the RL-designed and linear algorithms, respectively. The statistics is collected from solving 10^5 random 3-SAT problem instances using the corresponding quantum algorithms. The error bar represents the statistical error according to the bootstrap method. The infidelity is rescaled by taking its average as a unit. The infidelity distribution from the linear algorithm shown in (c) resembles a Wigner-Dyson type, whereas the distribution from the RL algorithm in (b) strongly deviates from that. In this plot we choose the adiabatic time $T = 6$, and the total bit number $N_b = 10$.

Summary and Discussion

In this work we report a reinforcement learning approach for automated quantum adiabatic algorithm design. We find apparent advantage of the RL approach over the conventional quantum adiabatic algorithms in Grover search and 3-SAT problems. The surprising transferability found in the application of the RL-approach to the 3-SAT problems suggests the RL-designed algorithm trained on relatively-smaller size problems is applicable to larger sizes, which is both practically useful and theoretically inspiring in considering the complexity scaling. We expect this aspect can be further improved by combining with transfer learning techniques. The performance of RL enabled automated adiabatic algorithm design is expected to be systematically improvable by using more resources for training on a larger set of problem instances. The performance of our approach can also be improved by introducing additional Hamiltonian terms that vanish at $t = 0$ and $t = T$, which would easily fit into the framework proposed here. Given its flexibility, our proposing architecture is expected to be applicable as well to the design of noisy resilient quantum algorithms by training on a noisy quantum computer.

One important issue of our RL-enabled algorithm design approach beyond the present scope is to analyze the precise complexity of the RL-designed algorithm, which is of great theoretical interest by itself and is worth future investigation. We expect the RL-designed quantum adiabatic algorithm may inspire novel circuit algorithms as well given the established complexity-equivalence be-

tween the two.

Methods

The reinforcement learning process. In our reinforcement learning of quantum adiabatic algorithms, the Q-table which evaluates the different Hamiltonian paths, is approximated by a deep neural network, $Q(\mathbf{b}, a; \theta)$, whose parameters θ are determined through a supervised learning process, with data generated from the RL-agent exploring the Hamiltonian path space. The exploration process follows a policy $\pi(a|\mathbf{b})$ which describes the probability of choosing action a at a path state \mathbf{b} . In the learning process, we use a ϵ -greedy policy in which with a probability $1 - \epsilon$ all actions are randomly selected at equal weight, and the action with maximal $Q(\mathbf{b}, a; \theta)$ value is chosen with an extra probability ϵ . This parameter ϵ is slowly varied from 0 to 90% in the learning process. We run cycles of this ϵ -greedy learning process to ensure convergence of the Q-table, which is analogous to the reannealing approach in simulated annealing method. At each step of RL exploration, the neural network is trained by varying the θ parameters to solve an iteration problem,

$$Q(\mathbf{b}, a; \theta) = r(a(\mathbf{b})) + \gamma \max_{a'} [Q(a(\mathbf{b}), a'; \theta_-)]. \quad (5)$$

The training data is generated from the memory \mathcal{M} that stores the path-states \mathbf{b} , actions a , and the corresponding rewards $r(a(\mathbf{b}))$ that the RL agent has explored. The parameters θ_- are only updated to θ every W steps (W is set to be 50 here), to deliberately slow down the iteration

process for stabilization purpose. This approach has been used in Ref. 32, and follows a standard approach to stabilize nonlinear iteration problems. When the iteration converges, $Q(\mathbf{b}, a; \theta)$ satisfies the Bellman equation [31].

After the Q-table converges, we let the agent update the path-state \mathbf{b} until it stabilizes, according to the ε -greedy policy with ε increased from 90% to 100% slowly.

Sampling 3-SAT problem instances. Given a total number N_b of boolean bits z_q , different 3-SAT problem instances correspond to different choices of three-bit combinations \mathbf{q}_i in each clause C_i , and different choices of the truth table of each clause defined to be $\mathbf{z}_{i\alpha} = (z^{(1)}, z^{(2)}, z^{(3)})$ in the main text. Since we aim at a quantum adiabatic algorithm generically applicable, we randomly sample the problem instances $\{\mathbf{q}_i, \mathbf{z}_i\}$ according to the definition of 3-SAT problem and take the averaged energy of the final quantum state of the adiabatic evolution to assign the reward of a path-state \mathbf{b} . It is worth noting here that the choice for the truth table is not completely random, and that for one clause in the 3-SAT problem, there are eight possibilities of choosing the truth table corresponding to the eight possibilities of constructing the clause. The size of the sampling space grows polynomially with N_b and exponentially with N_C .

Acknowledgement

J.L. acknowledges helpful discussion with Xiuze Luo. This work is supported by National Program on Key Basic Research Project of China under Grant No. 2017YFA0304204, National Natural Science Foundation of China under Grants No. 117740067, and the Thousand-Youth-Talent Program of China.

Author information

The first two authors J.L. and Z.Y.L. contribute equally to this work. Correspondence and requests for material should be sent to xiaopeng.li@fudan.edu.cn.

* xiaopeng.li@fudan.edu.cn

- [1] Preskill, J. Quantum computing and the entanglement frontier. *arXiv preprint arXiv:1203.5813* (2012).
- [2] Harrow, A. W. & Montanaro, A. Quantum computational supremacy. *Nature* **549**, 203 (2017).
- [3] Lund, A., Bremner, M. J. & Ralph, T. Quantum sampling problems, bosonsampling and quantum supremacy. *npj Quantum Information* **3**, 15 (2017).
- [4] Bloch, I. Quantum simulations come of age. *Nature Physics* **14**, 1159 (2018).
- [5] Shor, P. W. Polynomial-time algorithms for prime factorization and discrete logarithms on a quantum computer. *SIAM review* **41**, 303–332 (1999).
- [6] Nielsen, M. A. & Chuang, I. Quantum computation and quantum information (2002).
- [7] Farhi, E. *et al.* A quantum adiabatic evolution algorithm applied to random instances of an np-complete problem. *Science* **292**, 472–475 (2001). <http://science.sciencemag.org/content/292/5516/472.full.pdf>.
- [8] Albash, T. & Lidar, D. A. Adiabatic quantum computation. *Rev. Mod. Phys.* **90**, 015002 (2018).
- [9] Devoret, M. H. & Schoelkopf, R. J. Superconducting circuits for quantum information: an outlook. *Science* **339**, 1169–1174 (2013).
- [10] Otterbach, J. *et al.* Unsupervised machine learning on a hybrid quantum computer. *arXiv preprint arXiv:1712.05771* (2017).
- [11] Ibm q experience. <https://quantumexperience.ng.bluemix.net>.
- [12] King, A. D. *et al.* Observation of topological phenomena in a programmable lattice of 1,800 qubits. *Nature* **560**, 456 (2018).
- [13] Neill, C. *et al.* A blueprint for demonstrating quantum supremacy with superconducting qubits. *Science* **360**, 195–199 (2018).
- [14] Gong, M. *et al.* Genuine 12-qubit entanglement on a superconducting quantum processor. *arXiv preprint arXiv:1811.02292* (2018).
- [15] Wang, H. *et al.* High-efficiency multiphoton boson sampling. *Nature Photonics* **11**, 361 (2017).
- [16] Lored, J. C. *et al.* Boson sampling with single-photon fock states from a bright solid-state source. *Phys. Rev. Lett.* **118**, 130503 (2017).
- [17] Wu, J. *et al.* A benchmark test of boson sampling on tianhe-2 supercomputer. *National Science Review* **5**, 715–720 (2018).
- [18] Brown, K. R., Kim, J. & Monroe, C. Co-designing a scalable quantum computer with trapped atomic ions. *npj Quantum Information* **2**, 16034 (2016).
- [19] Bernien, H. *et al.* Probing many-body dynamics on a 51-atom quantum simulator. *Nature* **551**, 579 (2017).
- [20] Wu, T.-Y., Kumar, A., Mejia, F. G. & Weiss, D. S. Stern-gerlach detection of neutral atom qubits in a state dependent optical lattice. *arXiv preprint arXiv:1809.09197* (2018).
- [21] Van Dam, W., Mosca, M. & Vazirani, U. How powerful is adiabatic quantum computation? In *Foundations of Computer Science, 2001. Proceedings. 42nd IEEE Symposium on*, 279–287 (IEEE, 2001).
- [22] Aharonov, D. *et al.* Adiabatic quantum computation is equivalent to standard quantum computation. *SIAM review* **50**, 755–787 (2008).
- [23] Yu, H., Huang, Y. & Wu, B. Exact equivalence between quantum adiabatic algorithm and quantum circuit algorithm. *Chinese Physics Letters* **35**, 110303 (2018).
- [24] Roland, J. & Cerf, N. J. Quantum search by local adiabatic evolution. *Phys. Rev. A* **65**, 042308 (2002).
- [25] Preskill, J. Quantum Computing in the NISQ era and be-

- yond. *Quantum* **2**, 79 (2018).
- [26] Bukov, M. *et al.* Reinforcement learning in different phases of quantum control. *Phys. Rev. X* **8**, 031086 (2018).
 - [27] Berry, M. V. Transitionless quantum driving. *Journal of Physics A: Mathematical and Theoretical* **42**, 365303 (2009).
 - [28] Chen, X., Lizuain, I., Ruschhaupt, A., Guéry-Odelin, D. & Muga, J. Shortcut to adiabatic passage in two-and three-level atoms. *Physical review letters* **105**, 123003 (2010).
 - [29] Yang, X.-C., Yung, M.-H. & Wang, X. Neural-network-designed pulse sequences for robust control of singlet-triplet qubits. *Phys. Rev. A* **97**, 042324 (2018).
 - [30] Niu, M. Y., Boixo, S., Smelyanskiy, V. & Neven, H. Universal quantum control through deep reinforcement learning. *arXiv preprint arXiv:1803.01857* (2018).
 - [31] Bellman, R. On the theory of dynamic programming. *Proceedings of the National Academy of Sciences* **38**, 716–719 (1952).
 - [32] Mnih, V. *et al.* Human-level control through deep reinforcement learning. *Nature* **518**, 529–533 (2015).
 - [33] Grover, L. K. A fast quantum mechanical algorithm for database search. In *Proceedings of the twenty-eighth annual ACM symposium on Theory of computing*, 212–219 (ACM, 1996).
 - [34] Farhi, E. & Gutmann, S. Analog analogue of a digital quantum computation. *Phys. Rev. A* **57**, 2403–2406 (1998).